2007

Electrostatic Charge Polarity Effect on Respiratory Deposition in the Glass Bead Tracheobronchial Airways Model

Mohammed Ali
The University of Texas at Tyler, mohammedali@uttyler.edu

Malay K. Mazumder

Rama N. Reddy

Mariofanna Milanova

Jing Zhang

See next page for additional authors

Author
Mohammed Ali, Malay K. Mazumder, Rama N. Reddy, Mariofanna Milanova, Jing Zhang, and Alexandru S. Biris

Electrostatic Charge Polarity Effect on Respiratory Deposition in the Glass Bead Tracheobronchial Airways Model

MOHAMMED ALI[1,2], MALAY K. MAZUMDER[1], RAMA N. REDDY[1], MARIOFANNA MILANOVA[1], JING ZHANG[1], AND ALEXANDRU S. BIRIS[1]

[1]*Donaghey College of Information Science and Systems Engineering, University of Arkansas at Little Rock ETAS 575, 2801 S. University Ave., Little Rock, AR 72204, USA*

[2]Correspondence: mxali@ualr.edu

Abstract.—The effects of unipolar and bipolar electrostatic charges on the deposition efficiency of therapeutic aerosols in the physical model of human tracheobronchial (TB) airways have been investigated. Respirable size aerosol particles were generated by a commonly prescribed and commercially available nebulizer and charged by a corona charger and then their size and charge distributions were characterized by an Electronic Single Particle Aerodynamic Relaxation Time analyzer to study the drug aerosol particles' deposition pattern. The experiments were performed with a glass bead tracheobronchial model (GBTBM) (physical model) which was designed and developed based upon widely used and adopted dichotomous lung morphometric data presented in the Ewald R. Weibel model. The model was validated with the respiratory deposition data predicted by the International Commission on Radiological Protection and the United States Pharmacopeia (USP) approved Andersen Cascade Impactor (ACI). Unipolarly and bipolarly charged particles were characterized for two configurations: a) without TB model in place and b) with TB model in place. Findings showed that the deposition of unipolarly charged particles was about 3 times of the bipolarly charged particles. It was also found that bioengineered therapeutic aerosols with good combinations of aerodynamic size and electrostatic charge are good candidates for the administration of respiratory medicinal drugs.

Key words.— unipolar electrostatic charges , bipolar electrostatic charges, therapeutic aerosols, tracheobronchial (TB) airways, human, nebulizer, corona charger, Electronic Single Particle Aerodynamic Relaxation Time, deposition efficiency, dichotomous lung morphometric data, Ewald R. Weibel model, International Commission on Radiological Protection, Andersen Cascade Impactor (ACI),

Introduction

A physical lung model that closely approximates the flow characteristics, surface area, and aerosol deposition patterns of the human lung could serve as a surrogate lung for *in-vitro* studies during the development of respiratory medicines and inhalation drug-delivery devices. The model will not only be beneficial for studies of regional lung deposition but will also eliminate safety issues and variabilities that are inherent with the use of human subjects. The human respiratory tract is an aerodynamic classifying system for inhaled particles (USEPA 1998). A sampling device can be used as a substitute for the respiratory tract as a particle collector, and it can effectively simulate the mechanisms of electromechanical deposition of the inhaled particles including inertial impaction, gravitational settling, interception, diffusion, and electrostatic force (Fig. 1).

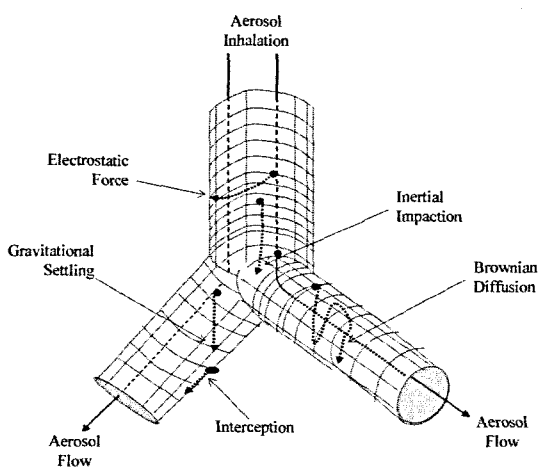

Fig. 1. Electromechanical deposition mechanisms of drug aerosols in the human lung.

Others have shown that a physical lung model simulated by a multi-layer granular bead filter provides a good approximation of the deposition detected in the *in vivo* experimental data (Altshuler et al. 1957). Gebhart and Heyder (1985a) developed the first granular bead filter to use as a surrogate for human subjects in their study of aerosol deposition. The filter consisted of a 30-cm long by 15.24-cm diameter acrylic cylinder, sealed by a cone at each end. The cone and cylinder were packed with 2.5-mm glass beads, resulting in airspace of approximately 2 L. Their model had several limitations. (A) It possessed a single passageway to simulate all respiratory airways though parameters of successive branching airways differ widely. (B) It was geometrically dissimilar with *in vivo* anatomy, and (C)

it was unable to test site-specific deposition for corresponding regions of the respiratory tract (Gao 1994).

Numerical analyses show that only 31% of 0.5 μm, 61% of 2 μm, and 63% of 5 μm drug particles deposit due to inertial impaction when the particles contain no elementary charge (Hinds 1998, p. 241). Besides, *in-vitro* investigation of metered dose inhaler and dry powder inhaler aerosols demonstrated that both respiratory drug delivery devices generate bipolarly charged particles (Glover and Chan 2003). Additionally, several studies have found that the electrostatic charge force influences particle deposition in the human lung along with other deposition mechanisms (Yu 1977, Gebhart and Heyder 1985b, Melandri et al. 1983, Hashish et al. 1994, Balachandran 1997, Bailey et al. 1998, Cohen et al. 1998).

In order to study the regional deposition of aerosol particles, it was necessary to design a multi-Stage models to simulate various regions of the lung anatomy. We designed and developed a physical tracheobronchial model using a USP metal throat, and 2 packed beds (Stages) of glass beads in the shape of a wedding cake (Figure 2), hereafter referred to as the Glass Bead Tracheobronchial Model (GBTBM). Since the GBTBM was constructed to mimic flow parameters and dimensions of the lung airways, it could simulate all 5 mechanisms of deposition of inhaled aerosol particles. The objectives of the current work were to (a) design and develop 2 layers of glass-bead filters to serve as a surrogate for tracheobronchial regions of respiratory airways, (b) investigate the particle deposition of pharmaceutical aerosols generated by a commercially available nebulizer, (c) validate the deposition efficiencies proposed by the International Commission on Radiological Protection (ICRP) deposition model, and (d) study the combined effects of aerosol particle size and charge on deposition in the GBTBM.

Materials and Methods

Mathematical Model.—A mathematical model was first developed to establish the basis for the design and construction of the GBTBM. Motion of a spherical particle in a given geometry is affected by the Stokes number *Stk*, particle size, flow Reynolds number Re_{flow}, and non-dimensional settling velocity (Zhang and Finlay 2005, Kim et al. 1994, Schlesinger et al. 1977, Chan & Schreck 1980). It is notable that Stokes number was originated from Stokes's law by solving the unsolvable Navier-Stokes equation based upon several assumptions (Hinds 1998). One of them was that the fluid should be incompressible, which is unlikely in case of drug aerosols. Additionally, in practice, Stokes law is restricted to situations in which flow Reynolds number is less than 1.0 (Hinds 1998). For an inhalation rate of 28.3 L/min, the flow Reynolds number in the tracheobronchial region is very high ($Re_{flow} >> 1.0$). Therefore, the simulation of Stokes number in this study was not considered. Besides, like an asthmatic patient the similar kind of drug aerosols and inhalation rate were used in the GBTBM experiments, which conform that both particle size and non-dimensional settling velocity were also simulated as well. Since the flow Reynolds number determines the nature of the flow, it can simulate the characteristics of 2 fluid flows and the flow profiles irrespective of the actual dimensions of the aerosol flows. Therefore, various regions of the lung can be classified according to the Reynolds numbers of the air flows in the respiratory airways for a given inhalation flow rate. Our calculations, beginning from the Reynolds numbers can be used to calculate the diameter and the number of glass beads for each Stage. Mathematically, the Reynolds number of a fluid flow can be determined from Equation 1.

$$Re = \frac{2 D_b v_s \tilde{n}}{3 \grave{\imath} (1 - \mathring{a})} \qquad (1)$$

where Re = Reynolds number, D_b = packed bed diameter, v_s = superficial velocity through the pipe, ρ = aerosol particle density, μ = aerosol viscosity, and ε = bed porosity. The other parameters of the GBTBM were calculated from Equations 2 – 6.

(2) Superficial velocity due to the packed bed, $v_s = v_m \varepsilon$

(3) Volumetric flow rate through the Stage, $q_v = (\pi/4) D^2 v_m$

(4) Volume of glass beads, $V_g = (\pi/4) D^2 L(1 - \varepsilon)$

(5) Number of beads, $n = V_g / (\pi/6) d_g^3$

(6) Total surface area of the beads = $n\pi d_g^2$

Where v_m is the average velocity of aerosol flow through the packed bed an approximation based on the range of air velocity from Weibel's model, d_g = glass bead diameter, D = bed (Stage) diameter, and L = Stage length. Table 1 shows the design parameters of the GBTBM Stages 1 and 2.

Table 1. Summary of the design parameters of the of the glass bead tracheobronchial model.

Design parameter	Stage 1: Trachea	Stage 2: Main and Lobar Bronchus
Flow rate through Stage, Q, l/min	28.3	28.3
Bed Porosity, e	0.38	0.36
Mean velocity on packed bed, vm, cm/s	383.5	234.53
Superficial velocity through Stage, vs, cm/s	145.73	84.43
Stage diameter, D, cm	2.03	2.67
Stage Length, L, cm	18.875	18.733
Volume of the inside Stage, Vp, cm^3	61.09	104.65
Total volume of beads needed, Vg, cm^3	37.88	66.98
Bead diameter, dg, cm	1.37	1.1
Number of glass beads, n	28	50
Surface area of packed bed, cm^2	165.88	293.33
Reynolds number of packed bed, Re	2135	1198
Reynolds number in Weibel's model, Re	2213	1241

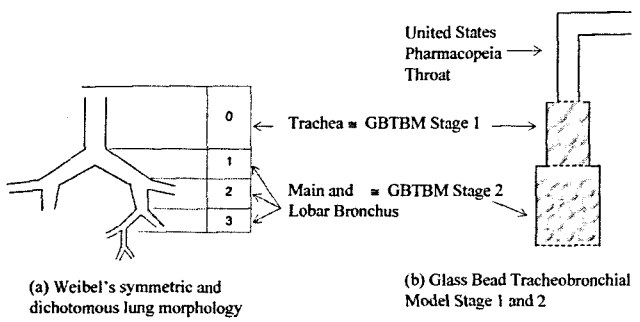

Fig. 2. Two Stage glass bead tracheobronchial model simulates trachea, main, and lobar bronchus regions of the human respiratory system.

Glass Bead Tracheobronchial Physical Model.—Figure 2 shows the GBTBM and the corresponding simulated regions of the human respiratory tract. The dimensions of the lung airway regions were based upon widely used and adopted symmetric and dichotomous lung morphological data in Ewald R. Weibel lung model with some modification due to the more recently published data of Horsfield et al. (Weibel 1963, Horsfield et al. 1971).

Weibel's model portrays the common and standard understanding of human lung anatomy. It divides the human respiratory tract into 24 generations (from G0 to G23). Since inception, it has been regarded as a detailed anatomical approach to lung morphology, the model was tested and validated with experimental results. Weibel's morphometric data provide specific length, diameter, area, and volume for each generation. In our model, Stage 1 simulated the trachea, the first generation (G0) of the respiratory tract (Figure 2). Stage 2 simulated the main and lobar bronchi, the second, third, and fourth generations (G1–G3) of the respiratory tract. Each of these Stages was stacked one on top of the other with wire-mesh supports to maintain the flow of aerosol for uniform distribution over each Stage. Each lung region was represented by a glass-bead-packed bed with a diameter that simulated the surface area of the region and the flow Reynolds number at an inspiratory flow rate of 28.3 l/min.

Ideally, each generation of the respiratory system should be simulated by a single bed of glass beads of relevant size and thickness. However, for expediency in constructing the physical model, three generations of bronchi were represented by Stage 2 in such a way that particle deposition should not have changed significantly. In order to obtain a Reynolds number as close as possible to that of the tracheal region (2235), we made the surface area of packed bed in Stage 1 166 cm^2. The surface area of packed bed in Stage 2 was made 293 cm^2 to achieve a Reynolds number (1241) as close as possible to that of the bronchial region. The circular cylinders of the Stages 1 and 2 were made from 2.03-cm and 2.67-cm PVC pipes, respectively (American Valve™, 3/4" and 1" Fix-It Coupling PVC, Model: P232, Lowe's Companies, Inc. North Wilkesboro, NC). The sizes of the glass beads were based upon the required bed porosity in order to achieve the closest possible Reynolds numbers for a fixed inhalation flow rate (Glen Mills Inc., Clifton, NJ). The copper wire mesh supported the glass beads and maintained a uniform flow (TWP Inc., Berkeley, CA).

Experimental Setup.—Figure 3 depicts the experimental system, which consisted of several components addressed below.

1. In order to generate therapeutic grade aerosols, we used a nebulizer (PARI LC Plus®, Midlothian, VA) and sodium chloride solution (7 g/ml) aerosols with mass median aerodynamic diameters (MMAD) ranging between 4.0 μm and 5.5 μm.

2. A corona charger was used to charge aerosols before inhalation through the GBTBM. The charger also acted as an aerosol holding chamber (AHC) with dimensions of 21 cm x 18 cm x 21 cm (LxWx H).

3. The USP induction port was used for introducing aerosols into the GBTBM. Manufacturers also specify the use of such a USP port for introducing aerosols into the Andersen Cascade Impactor **(e.g., 8 Stage Non-Viable Cascade Impactor of New Star Environmental LLC, Roswell, GA).**

4. The Glass Bead Tracheobronchial Model was placed between the USP port and the aerosol isokinetic sampling chamber (ISC). The Stages 1 and 2 could be separated or connected (together or individually) with the USP port and the ISC.

5. The Electronic Single Particle Aerodynamic Relaxation Time (ESPART) analyzer was used to measure aerodynamic sizes and electrostatic charges in real time (Mazumder and Ware 1987). Its working principle was by Mazumder et al. (1989).

6. An aerosol isokinetic sampling chamber (ISC) was used to facilitate the characterization of aerosols isokinetically (Figure 3). The suction mouth of the ESPART analyzer was placed at the center of the chamber and always pointed in the direction opposite of the aerosol flow.

External clean and dry air (18.3 l/min) and nebulized aerosol (10 l/min) were delivered to the AHC to simulate a light physical activity inhalation flow rate of 28.3 l/min through the GBTBM. The flow rate was measured using an Extech Heavy Duty Hot Wire Thermo-Anemometer™ (Extech Instruments, Waltham, Massachusetts, USA). The constant inhalation rate of 28.3 l/min served two purposes. (1) The manufacturer-specified flow rate for a Mark II Andersen Cascade Impactor (ACI) is 28.3 L/m, which enabled GBTBM comparability with the ACI. (2) The vacuum pump and the ESPART could have drawn 27.3 l/min and 1 l/min, respectively. The environmental conditions such as lab temperature (20°C) and humidity (51.2%) were recorded using Testo625™ (Testo GmbH & Co., Lenzkirch, Germany) thermo-anemometer.

In order to find the aerosol particle aerodynamic size, the electrostatic charge distributions and the charging effects upon

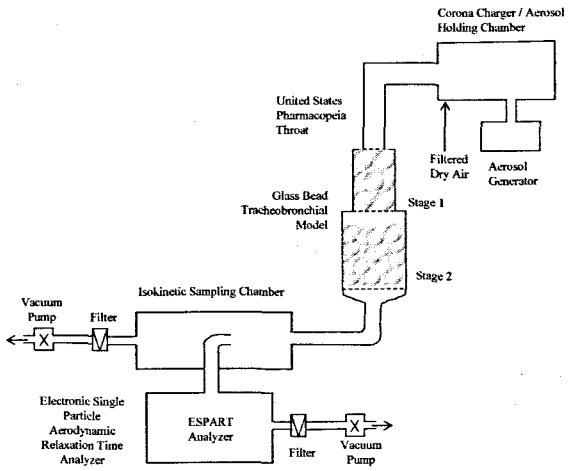

Fig. 3. Schematic of the experimental arrangement designed to measure aerodynamic diameters and electrostatic charges of the aerosol particles with and without passing through the glass bead tracheobronchial model.

particle deposition in the GBTBM, the investigation was divided into 6 experimental treatments of the aerosol:

(1a) not charged or passed through the GBTBM (the charger was OFF and the USP port was directly connected to ISC)

(1b) charged but not passed through the GBTBM (the charger was ON and the USP port was directly connected to ISC)

(2a) not charged but passed through the GBTBM Stage 1(the charger was OFF and the USP port was connected to the GBTBM Stage 1)

(2b) charged and passed through the GBTBM Stage 1 (charger was ON and the USP port was connected to the GBTBM Stage 1)

(3a) not charged but passed through the GBTBM Stages 1 and 2 (the charger was OFF and the USP port was connected to the GBTBM Stages 1 and 2) and

(3.b) charged and passed through the GBTBM Stages 1 and 2 (charger was ON and the USP port was connected to the GBTBM Stages 1 and 2).

Before starting each run of the experiment, the aerosol-sampling chamber and the charger were cleaned thoroughly. The GBTBM was washed with distilled water. The high-voltage power supply was adjustable and the corona charger could either be turned OFF or ON. The generation and sampling of the aerosol particles started simultaneously. Each run continued for 5 minutes and was then stopped. The AHC, USP port, GBTBM, and the ISC were cleaned again. To ensure our assumption of equal particle losses each time in the USP induction port (throat), the port was in place for all of the scenarios described above. The procedure was repeated for 10 consecutive runs for each treatment. The sizes and charge distributions were measured in each case. Raw data was acquired through LabVIEW™ (National Instruments, Austin, TX, USA) and mined by Aerosol Particle Data Analyzer software (developed at the Aerosol Drug Delivery Research Lab of the University of Arkansas at Little Rock, Little Rock, AR, USA). Our study focused on particles in the aerodynamic diameter range of 0.5 μm - 10 μm with a geometric standard deviation greater than 1.5 because therapeutic aerosols known at present or anticipated to be of primary practical importance for predicting lung deposition have aerodynamic diameters in the range of 0.5 μm - 10 μm (Swift 1996).

Results

We assumed that the both Stages of the glass bead tracheobronchial model would operate on 1 basic principle. Particles whose inertia exceeds a certain value (cutoff size) would be unable to follow the streamlines and will impact upon the packed bed. In addition, particles would deposit on the bead surfaces due to diffusion, sedimentation, interception, and electrostatic force. Thus, each Stage of the GBTBM would separate aerosol particles into 2 size ranges; particles larger than the cutoff size will be removed from the aerosol stream, and particles smaller than that size will remain airborne and pass through the Stage. As a result, each Stage of the GBTBM will be characterized by a cutoff diameter. Figure 4 shows the cutoff curves, or collection-efficiency curves, of the glass bead tracheobronchial model Stages 1 and 2.

The deposition fraction will be defined as the ratio of the number of particles removed from the aerosol (i.e., deposited) while traveling through the GBTBM to the number of particles originally entering it. Table 2 shows the normalized data from

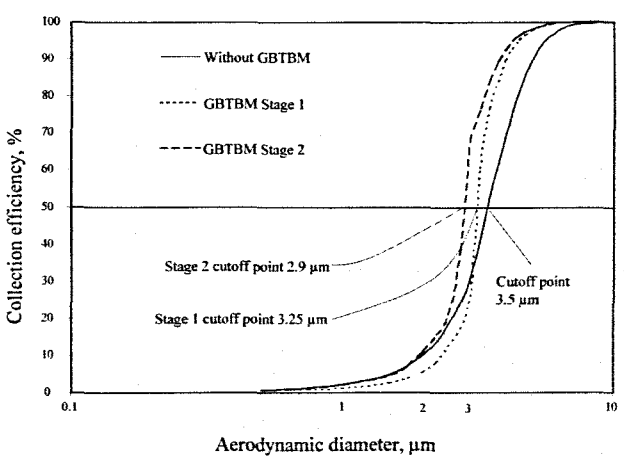

Fig. 4. Comparison of the aerosol particle collection efficiency curves of the glass bead tracheobronchial model Stages 1, 2 and without the GBTBM.

10 runs for uncharged particles for experimental scenarios 1.a, 2.a, and 3.a. Table 2 also summarizes the coefficient of variation (COV), count median aerodynamic diameter (CMAD), mass median aerodynamic diameter (MMAD), and the deposition fraction of uncharged particles in the GBTBM Stages 1 and 2.

Table 2. Summary of the normalized data of uncharged particle and deposition efficiency in the glass bead tracheobronchial model (GBTBM).

Experimental Scenario[1]	Uncharged Particle	Charged particle	CMAD[3]	MMAD[4]	DF[6]
	COV[2]	+ ve	(μm)	(μm)	
		- ve	SD[5]	SD[5]	
(1.a) By-passed GBTBM Stages	6470	21	3.21	4.31	N/A
	0.01	8	0.1	0.19	
		13			
(2.a) Inhaled through GBTBM Stage 1	5085	27	3.18	3.43	0.21
	0.002	14	0.005	0.03	
		13			
(3.a) Inhaled through GBTBM Stage 1 & 2	4466	47	3.08	3.51	0.31
	0.004	22	0.02	0.04	
		25			

[1]See Materials and Methods section.
[2]COV = coefficient of variation
[3]CMAD = count median aerodynamic diameter
[4]MMAD = mass median aerodynamic diameter
[5]SD = standard deviation
[6]DF = deposition fraction.

Figure 5 shows a comparison of the respiratory deposition fraction in the GBTBM airways to the respiratory deposition fraction in the ICRP model for the respirable range aerosol particles. Although the basic ICRP deposition curve was developed for particles in the size range of 0.001 μm – 100 μm, we have compared our GBTBM with the ICRP's respirable (therapeutic) size range (0.5 μm - 10 μm) portion only.

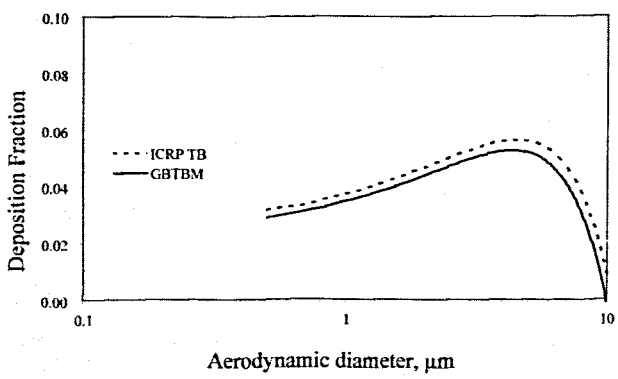

Fig. 5. Comparison of the respiratory deposition fraction of the glass bead tracheobronchial model airways and the International Commission on Radiological Protection tracheobronchial (ICRP TB) airways for the respirable range aerosol particles.

Table 3 shows the normalized data from 10 runs of charged particles for experimental treatments 1b and 3b. It also summarizes the coefficient of variation (COV), count median aerodynamic diameter (CMAD), mass median aerodynamic diameter (MMAD), electrostatic net charge-to-mass ratio, and the deposition fraction in the GBTBM Stages 1 and 2 combined.

Table 3. Summary of the normalized data of charged particle and deposition efficiency in the glass bead tracheobronchial model (GBTBM).

Experimental Scenario[1]	Charged Particle	Net Charge to mass ratio	CMAD[3]	MMAD[4]	DF[6]
	COV[2]	(μC/g)	(μm)	(μm)	
	+ ve		SD[5]	SD[5]	
	- ve				
(1.b) By-passed GBTBM Stages	3563	-19.84	2.25	4.17	N/A
	0.01		0.03	0.09	
	3				
	3560				
(3.b) Inhaled through GBTBM Stages (both Stage 1 and 2 were in place)	592	-7.06	2.63	6.25	0.83
	0.02		0.01	0.02	
	18				
	574				

[1]See Materials and Methods section.
[2]COV = coefficient of variation
[3]CMAD = count median aerodynamic diameter
[4]MMAD = mass median aerodynamic diameter
[5]SD = standard deviation
[6]DF = deposition fraction.

Figure 6 shows the comparison of the cumulative respiratory deposition fraction of bipolar-charged versus unipolar-charged aerosols in the GBTBM airways.

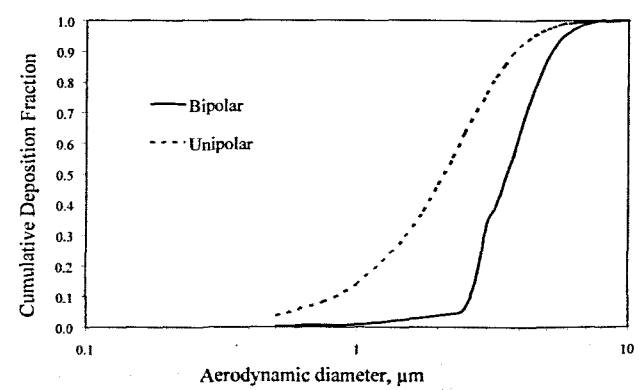

Fig. 6. Comparison of the respiratory deposition fraction of bipolar charged versus unipolar charged aerosols in the glass bead tracheobronchial model airways.

Discussion

In this study, we are reporting physical simulations of the tracheobronchial airways of the human lung were reported. We have demonstrated the model's design and development validity. Secondly, our model showed a consistency with the ICRP66 Model in particle deposition for particles in the therapeutic aerosol particle size range. Finally, it showed the deposition pattern of bipolar versus unipolar-charged aerosol particles in the GBTBM.

Validation of the Design and Development of the GBTBM.–A 2-Stage GBTBM was designed and developed to simulate the human respiratory tract Generation 0 (trachea, G0) and Generations 1, 2, and 3 (main and lobar bronchi, G1-G3), respectively. The first Stage simulated Reynolds number was 2135, which was in close approximation with the flow Reynolds number in the trachea of 2213 (ideal case) for an inhalation flow rate of 28.3 l/m. The second Stage simulated Reynolds number was 1198, which was also in close approximation with the average Reynolds number of 1241 for the first, second, and third bronchi for the given inhalation flow rate. However, for convenience in constructing the physical model and to achieve the closest possible flow parameters, the surface areas of the packed bead Stages were 5 and 17 times the *in vivo* surface areas, respectively. In spite of these differences in surface areas between the actual tracheobronchial morphology and the GBTBM, simulated depositions are in accordance with previous studies conducted by the ICRP (ICRP66 1994). The collection efficiency or cutoff points of the GBTBM Stages are in the range (Figure 4) that has been specified by the manufacturer of the ACI (NSE 2004).

Comparison with the ICRP66 TB Model.–Regional respiratory deposition predictions made by the ICRP Publication 66 (ICRP66 1994) are based upon both empirical analyses (Rudolf et al. 1990) and a theoretical model developed by Egan et al. (1989). The ICRP66 model takes into account particle parameters such as size, shape, and density, as well as anatomical parameters such as airway dimensions and flow rates. Our GBTBM was a physical model for *in-vitro* studies. In addition to all the considerations taken by ICRP66, we took into account the electrical properties of aerosols and environmental parameters (e.g., temperature, humidity). Although our model predicted deposition for each aerodynamic size about 5% lower, overall, results were fairly consistent with the ICRP depositions for the particle size range of 0.5 μm - 10 μm (Figure 5). The difference could be due to different assumptions and methods used in the derivation of the formulae such as, ICRP Model is an empirical lung deposition model which considered aerodynamic and thermodynamic deposition formulas to derive respiratory deposition of radionuclide particles, whereas our GBTBM is a physical model simulating integrated electromechanical deposition mechanisms as stated in Figure 1.

Comparison of the Charge Polarity Effect.–The respiratory deposition patterns of bipolarly charged (e.g., negligible net charge-to-mass ratio) particles clearly demonstrates the trend of unipolarly charged particles to be deposited in the upper airways (Figure 6). Data revealed that uncharged-particle-deposition efficiency in the GBTBM was 31% (Tables 3 and 4). In contrast the deposition efficiency was 83% when the particles were charged. The net charge-to-mass ratio also dropped from 19.84 μC/g (negative) to 7.06 μC/g (negative). Hence, there were some electrostatic force situations. First of all, the unipolarly charged particles induced greater space charge forces and mutual repulsion. As a result, particles came closer to the surfaces of the glass bead and were captured. This feature, which is due to electromagnetic forces, is consistent with Yu's (1977) theory and the experimental observations by Bailey et al. (1998). Secondly, since uncharged particles are without charge, electromagnetic forces have no effect on them. Furthermore, there were only a few (2%) bipolar symmetrically charged particles, they became neutralized over the course of travel through the Stages due to the Coulombic attractive forces among themselves. It was our observation that the aerosol particles with symmetrical bipolar charge distributions traversed efficiently through the tracheobronchial regions. We observed that the most efficient bipolar charged particles were in the size range of 1 μm - 3 μm, which showed the lowest deposition in the tracheobronchial region (Figure 6). This finding suggests that bioengineered therapeutic aerosols with good combinations of aerodynamic size and electrostatic charge are good candidates for the administration of pulmonary medicinal drugs.

Compared to the commonly used ACI aerodynamic classifying system, which provides a quick estimation for aerosol depositions, the GBTBM described in this paper offers a more detailed description of aerodynamic size and electrostatic charge distribution of the deposited particles (Figures 4, 5, and 6). Whereas the ACI Stages are made of electrically conductive materials, the GBTBM Stages are not. This is a limitation that can be overcome in the production of future GBTBMs by constructing Stage cylinders of similarly conductive materials.

Conclusions

A two-Stage GBTBM of the upper airways of the human lung has been designed, developed, and realized. It is comparable to the Mark II ACI. In addition, the GBTBM simulated by packed bed media is simple, inexpensive, and a prospective model for the *in-vitro* investigation of aerosolized drug delivery. The respirable size range for therapeutic aerosols deposition in the GBTBM is comparable with the mathematical and theoretical results reported in the ICRP66 model. Bipolar aerosol particles, or particles balanced with positive and negative polarity, pass through the tracheobronchial regions more successfully than the unipolar charged aerosol particles and provide better delivery to the bronchiolar and alveolar regions of the human lung. Our study is an important step in finding an alternative to the ACI, which is unable to simulate the interactive behaviors of deposition mechanisms in respiratory airways.

Literature Cited

Altshuler B, L Yarmus, ED Palmes, and N Nelson. 1957. Aerosol deposition in the human respiratory tract. I. Experimental procedures and total deposition. American Medical Association Archives of Industrial Health 15:293-303.

Bailey AG, AH Hashish, and TJ Williams. 1998. Drug delivery by inhalation of charged particles. Journal of Electrostatics 44:3-10.

Balachandran W. 1997. Control of drug aerosol in human airways using electrostatic forces. Journal of Electrostatics 40&41:579-584.

Chan TL and RM Schreck. 1980. Effect of the laryngeal get on particle deposition in the human trachea and upper bronchial airways. Journal of Aerosol Science 11:447-459.

Cohen BS, JQ Xiong, CP Fang, and W Li. 1998. Deposition of charged particles on lung airways. Health Physics 74(5):554-560.

Egan MJ, W Nixon, NI Robinson, A James, and RF Phalen. 1989. Inhaled aerosol transport and deposition calculations for the ICRP task group. Journal of Aerosol Science 20:1305-1308.

Gao S. 1994. Development of two-component packed granular filters with triboelectric enhancement. PhD Dissertation Little Rock (AR): University of Arkansas at Little Rock. 87 p.

Gebhart J and J Heyder. 1985a. Removal of aerosol particles from stationary air within porous media. Journal of Aerosol Science 16(2):175-187.

Gebhart J and J Heyder. 1985b. On practical significance of electrostatic lung deposition of isometric and fibrous aerosols. Journal of Aerosol Science 16(6):511-519.

Glover W and HK Chan. 2003. Electrostatic charge characterization of pharmaceutical aerosols using electrical low-power impaction (ELPI). Journal of Aerosol Science 35:755-764.

Hashish AH, AG Bailey, and TJ Williams. 1994. Selective deposition of pulsed charged aerosols in the human lung. Journal of Aerosol Medicine 7(2):167-171.

Hinds WC. 1998. Aerosol Technology: properties, behavior and measurement of airborne particles. 2nd ed. New York: John Wiley & Sons Inc. 483 p.

Horsfield K, G Dart, DE Olson, GF Filley, and G Cumming. 1971. Models of the human bronchial tree. Journal of Applied Physiology 31(2):207-217.

[ICRP] International Commission on Radiological Protection. 1994. Human Respiratory Tract Model for Radiological Protection, ICRP Publication 66. New York: Elsevier Sci. Inc. 433 p.

Kim CS, DM Fisher, DJ Lutz, and TR Gerrityet. 1994. Deposition of inhaled particles in bifurcating airway models with varying airway geometry. Journal of Aerosol Science 25:567-581.

Mazumder MK and RE Ware. 1987. Aerosol particles charge and size analyzer, US Patent number 4633714.

Mazumder MK, JD Wilson, DL Wankum, R Cole, GM Northrop, LT Neidhardt, and TB Martonen. 1989. Dual laser Doppler system for real-time simultaneous characterization of aerosols by size and concentration. *In*: Crapo JD, editor. Lung Dosimetry. San Diego (CA): Academic Press. p 211- 234.

Melandri C, G Tarroni, V Prodi, TD Zaiacomo, M Formignani, and C Lombardi. 1983. Deposition of charged particles in the human airways. Journal of Aerosol Science 14(5):657-669.

[NSE] New Star Environmental LLC. 2004. Instruction Manual for 8 Stage Non-Viable Cascade Impactor. Roswell (GA): NSE. 7 p.

Rudolf G, R Kobrich, and W Stahlhofen. 1990. Modeling and algebraic formulation of regional aerosol deposition in man. Journal of Aerosol Science 21:S403-S406.

Schlesinger RB, DE Bohning, TL Chan, and M Lippmann. 1977. Particle deposition in a hollow cast of the human tracheobronchial tree. Journal of Aerosol Science 8:429-445.

Swift DL. 1996. Use of mathematical aerosol deposition models in predicting the distribution of inhaled therapeutic aerosols. *In*: Hickey AJ, editor. Inhalation Aerosols. New York: Marcel Dekker. p 51-81.

[US EPA] US Environmental Protection Agency. 1998. Guidelines on speciated particulate monitoring. Draft 3. Research Triangle Park (NC): USEPA. 3-1 p. Available from: http://www.epa.gov/ttn/amtic/files/ambient/pm25/spec/drispec.pdf.

Weibel ER. 1963. Morphometry of the Human Lung. Berlin: Springer-Verlag. 340 p.

Yu CP. 1977. Precipitation of unipolarly charged particles in cylindrical and spherical vessels. Journal Aerosol Science 8:237-241.

Zhang Y and WH Finlay. 2005. Experimental measurements of particle deposition in three proximal lung bifurcation models with an idealized mouth-throat. Journal of Aerosol Medicine 18(4):460-473.